

# Stabilizing the Frank-Kasper Phases via Binary Blends of AB Diblock Copolymers

Meijiao Liu,<sup>†,‡,¶</sup> Yicheng Qiang,<sup>†</sup> Weihua Li,<sup>\*,†</sup> Feng Qiu,<sup>†</sup> and An-Chang Shi<sup>\*,‡</sup>

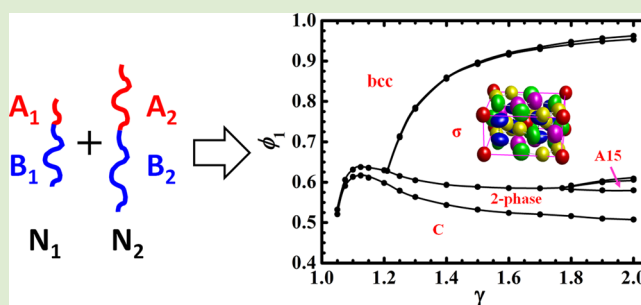
<sup>†</sup>State Key Laboratory of Molecular Engineering of Polymers, Collaborative Innovation Center of Polymers and Polymer Composite Materials, Department of Macromolecular Science, Fudan University, Shanghai 200433, China

<sup>‡</sup>Department of Physics and Astronomy, McMaster University, Hamilton, Ontario, Canada L8S 4M1

<sup>¶</sup>Department of Chemistry, Key Laboratory of Advanced Textile Materials and Manufacturing Technology of Education Ministry, Zhejiang Sci-Tech University, Hangzhou 310018, China

## S Supporting Information

**ABSTRACT:** The emergence of the complex Frank-Kasper phases from binary mixtures of AB diblock copolymers is studied using the self-consistent field theory. The relative stability of different ordered phases, including the Frank-Kasper  $\sigma$  and A15 phases containing nonspherical minority domains with different sizes, is examined by a comparison of their free energy. The resulting phase diagrams reveal that the  $\sigma$  phase occupies a large region in the phase space of the system. The formation mechanism of the  $\sigma$  phase is elucidated by the distribution of the two diblock copolymers with different lengths and compositions. In particular, the segregation of the two types of copolymers, occurring among different domains and within each domain, provides a mechanism to regulate the size and shape of the minority domains, thus enhancing the stability of the Frank-Kasper phases. These findings provide insight into understanding the formation of the Frank-Kasper phases in soft matter systems and a simple route to obtain complex ordered phases using block copolymer blends.



The Frank-Kasper (FK) phases, also known as tetrahedrally closed packed phases, are a class of complex crystalline structures possessing large unit cells with many nonequivalent lattice sites within the cell.<sup>1</sup> One example is the FK  $\sigma$  phase, which has a giant unit cell containing 30 lattice sites belonging to five nonequivalent types (Figure 1). Initially, the FK phases were discovered in metallic alloys.<sup>2</sup> Recently, the FK phases

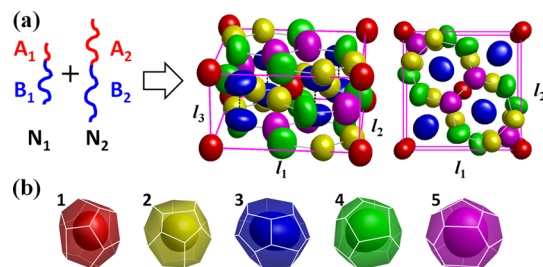


**Figure 1.** (a) Oblique (left) and top (right) views of a unit cell for the  $\sigma$  phase from the binary blend of AB diblock copolymers with lengths  $N_1$  and  $N_2$ , respectively.  $\gamma = N_2/N_1$  is introduced to quantify the length ratio. The minority domains within the cell are obtained from isosurface plots of  $\phi_A(\mathbf{r}) = 0.5$ . The five types of domains are shown in different colors. The cell dimensions are  $l_1 = l_2 \neq l_3$ , as dictated by the  $P4_2/mmm$  symmetry of the structure. (b) Plots of the five polyhedral Wigner-Seitz cells of the five types of domains.

have been attracting renewed attention due to the observation of them in soft condensed matter systems including amphiphilic superbranched liquid crystals,<sup>3,4</sup> molecular amphiphiles composed of nanoscale cubes,<sup>5</sup> linear tetrablock terpolymer,<sup>6</sup> and conformational-asymmetric diblock copolymers.<sup>7</sup> These studies have motivated a number of theoretical studies.<sup>8–12</sup> Understanding the formation mechanism of the FK phases in soft matter systems presents a challenge to the soft matter community.<sup>3,6–11,13,14</sup>

The FK phases are originally found in metallic alloys with large and small atoms.<sup>1</sup> It is natural to expect that this rule applies to soft matter systems as well, in which the soft FK phases would possess large and small domains (Figure 1).<sup>8–11</sup> In an insightful paper,<sup>7</sup> Lee et al. argued that the break of the spherical symmetry of the minority domains holds the key to understand the formation of domains with different nonspherical shapes. This mechanism stems from the competition between the tendency to form spherical domains and the need to uniformly fill the space under the constraint of the crystalline lattice, resulting in the formation of different spherical phases. Furthermore, they proposed that the transition from BCC to the FK- $\sigma$  phase is mediated by mass exchange between

Received: September 7, 2016

Accepted: September 30, 2016

Published: October 3, 2016

domains, resulting in the favorable distribution of domain sizes and shapes. Based on these arguments, it has been established that the deformability of the minority domains could be enhanced by forming large minority domains, whereas large domains could be realized in conformation-asymmetric diblock copolymers<sup>8,9,11</sup> or in multiblock copolymers.<sup>6,7,10,12,14</sup> A general rule for the self-assembly of soft FK phases emerged from these studies is the formation of minority domains of different *size* and *shape* accommodating the geometrical environment of the complex crystalline lattices with non-equivalent lattice sites. On the other hand, mechanisms for the formation of nonspherical domains of different sizes have not been clearly identified.

In this letter, the formation of the FK phases from binary mixtures of AB diblock copolymers with different lengths and compositions is studied theoretically. The phase behavior of binary mixtures of AB diblock copolymers has attracted considerable experimental<sup>15–17</sup> and theoretical<sup>18–20</sup> attention in the past years. The previous studies demonstrated that diblock copolymer blends exhibit complex phase behavior, however, most of them focused on the commonly observed diblock copolymer phases. The possibility of complex spherical phases such as the FK  $\sigma$  and A15 had never been explored. The current study reveals that, with proper chain lengths and compositions, the FK phases occupy a large region in the phase space (Figure 2). Therefore, the self-assembly of this simple system provides a novel route to stabilize the complex FK

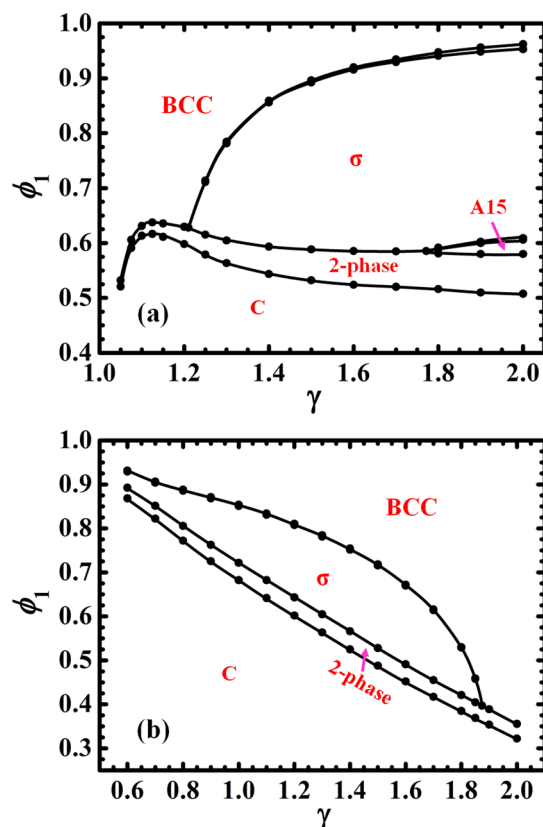


**Figure 2.** Phase diagrams in the  $\gamma$ – $\phi_1$  plane for the binary blends of AB diblock copolymers with  $\chi N = 40$  and  $f_1 = 0.15$ : (a)  $N_{B,2} = N_{B,1} = 0.85N$ ; (b)  $N_{A,2} = 0.45N$ . The symbols are the transition points determined from SCFT calculations. The solid lines are a guide for the eyes. The label of two-phase denotes the noticeable coexistence region of two neighboring phases.

phases, in particular the  $\sigma$  phase. More importantly, the study reveals an explicit mechanism to regulate the size and shape of the minority domains utilizing inhomogeneous distribution of the two types of diblock copolymers in the ordered structures (Figure 3). Specifically, the segregation of different diblocks

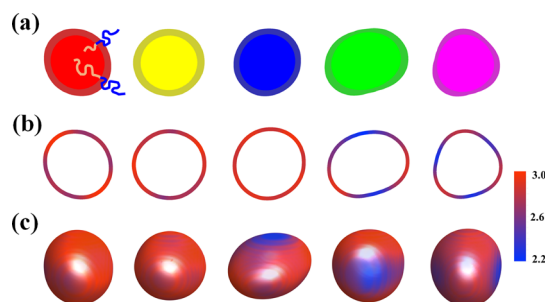


**Figure 3.** Density plots demonstrating the segregation of two different diblock copolymers within each domain for illustrating the mechanism of regulating the shape of minority domains: (a) segregation along the radial direction exhibiting anisotropic “core-shell” structures; (b, c) segregation at the interfaces shown by the two-dimensional and three-dimensional distribution of the joint points of the  $A_1B_1$  diblocks. The color spectrum from blue to red indicates the density of joint points of  $\phi_1 q(\mathbf{r}, f_1) q^\dagger(\mathbf{r}, f_1) / Q_1$  from low to high.

among the domains would lead to the formation of domains with different sizes, whereas their segregation within a domain would result in nonspherical domains.

The model system is a binary mixture of AB diblock copolymers,  $A_1B_1$  and  $A_2B_2$ , with chain length  $N_i$  and block ratio of the A-block  $f_i$  ( $i = 1, 2$ ). The A and B monomers have unique Kuhn length ( $b_\alpha$ ) and monomer density ( $\rho_{0\alpha}$ ), of which the pure conformation-symmetric diblock copolymer is not able to form the FK- $\sigma$  phase.<sup>9</sup>  $N_1 = N$  is chosen as a reference length, and  $\gamma = N_2/N_1$  quantifies the length ratio. The interaction between the A and B monomers is given by the Flory–Huggins parameter  $\chi$ . For this binary blend, its phase behavior depends on five parameters,  $\chi N$ ,  $f_1$ ,  $\gamma$ ,  $f_2$ , and  $\phi_1$ , where  $\phi_1$  is the volume fraction of  $A_1B_1$  in the mixture. We choose  $\chi N = 40$  and  $f_1 = 0.15$ , such that the equilibrium phase of  $A_1B_1$  is the BCC phase,<sup>21</sup> and examine the effects of  $\gamma$ ,  $f_2$ , and  $\phi_1$  on the phase behavior of the blends using self-consistent field theory (SCFT). Although SCFT is based on the Gaussian-chain model and the mean field treatment, it has become one of the most powerful methods to examine the phase behavior of inhomogeneous polymers.<sup>22,23</sup>

Specifically, extensive SCFT calculations have been carried out for two specific cases to illustrate the emergence and stabilization mechanism of the  $\sigma$  phase quantitatively. In the first case (Case 1), the two diblocks are assumed to have the same majority blocks ( $N_{B,1} = N_{B,2} = (1 - f_1)N = 0.85N$ ) and the phase behavior of the blends is examined in the  $N_{A,2}$ – $\phi_1$  or equivalently the  $\gamma$ – $\phi_1$  plane since  $N_{A,2} = (\gamma - 0.85)N$  in this case. In the second case (Case 2), the minority block of the second diblock is fixed at  $N_{A,2} = 0.45N$  and the phase behavior of the blends is examined in the  $N_{B,2}$ – $\phi_1$  or equivalently the  $\gamma$ – $\phi_1$  plane since  $N_{B,2} = (\gamma - 0.45)N$  in the second case. For these two cases, the phase diagrams in the  $\gamma$ – $\phi_1$  plane are shown in Figure 2, where the phase boundaries are determined using the pseudospectral method<sup>24,25</sup> of SCFT<sup>26,27</sup> formulated in the grand canonical ensemble.<sup>28</sup> Details of the SCFT formulation are provided in the Supporting Information.

The first noticeable result from the theoretical results (Figure 2) is that, with proper compositions, the  $\sigma$  phase occupies a large region in the phase space and the A15 phase could become stable as well. In the phase diagram of Figure 2a with  $N_{B,1} = N_{B,2} = 0.85N$  (Case 1),  $\gamma = 1$  corresponds to a diblock copolymer melt exhibiting a BCC phase at  $\chi N = 40$  and  $f_1 = 0.15$ . An increase in  $\gamma$  corresponds to cases with longer minority A-blocks since  $N_{A,2} = (\gamma - 0.85)N$  and  $N_{A,1} = 0.15N$ . It is expected that the addition of longer  $A_2$  blocks will swell the domains, resulting in anisotropic “core-shell” structures, thus drives BCC to transform into the  $\sigma$  phase. Indeed, when  $\gamma > 1.2$ , the  $\sigma$  phase starts to become stable. The stability region of the  $\sigma$  phase expands rapidly in the region of  $1.2 < \gamma < 1.5$ , reaching an approximately constant width of  $0.6 \lesssim \phi_1 \lesssim 0.95$  at  $\gamma \gtrsim 1.8$ . Meanwhile, the A15 phase starts to become stable just below the  $\sigma$  phase when  $\gamma \gtrsim 1.8$ .

In Case 2,  $N_{A,2} = 0.45N$  is intentionally chosen to be significantly longer than  $N_{A,1} = 0.15N$  to facilitate the formation of a “core-shell” distribution of the two A-blocks in each A domain. In the phase diagram of Figure 2b, an increase in  $\gamma$  corresponds to an increase in  $N_{B,2} = (\gamma - 0.45)N$ . A noticeable region of the  $\sigma$  phase, albeit narrower than that in Case 1, is again found in the phase diagram. This observation indicates that the length of the A-blocks provides a more effective mechanism to regulate the stability of the  $\sigma$  phase. Moreover, these results reveal that the addition of a small amount (a few percent) of the long  $A_2B_2$  is enough to drive the transition from BCC to the  $\sigma$  phase. This surprising theoretical prediction provides a novel and simple route to obtain the FK phases.

The FK phases are characterized by the presence of domains of different sizes and shapes within their unit cells. The nonsphericity of domains could be quantified by the isoperimetric quotient (IQ),  $IQ = 36\pi V^2/S^3$ , where  $V$  and  $S$  are the domain volume and area (Figure 1).<sup>7</sup> The formation of domains with different sizes and shapes from binary blends of AB diblocks stems from two mechanisms. The first and obvious mechanism is due to the different lengths of the minority A-blocks. The presence of long and short A-blocks would favor the formation of large domains with a core-shell structure via local segregation along the radial direction, in which the “core” is mainly constituted by the long A blocks, whereas the “shell” is mainly formed by the short A blocks. This core-shell structure could be quantitatively determined from the SCFT results, as shown in Figure 3a and Figure S2, in agreement with previous theoretical studies.<sup>18–20</sup> The formation of large minority domains would favor the formation of the FK phases. Indeed, larger polydispersity of the blocks in the cores than those in the coronas is roughly equivalent to the conformational asymmetry and, thus, reduces the entropy loss with chain stretching of the core, making it easier to deform. The similar effect of polydispersity has been proposed in binary brushes.<sup>29</sup>

The second, perhaps more subtle and more interesting, mechanism is due to the inhomogeneous distribution of the two diblocks. First of all, the concentration of the two diblocks in each domain could be different, providing a mechanism to regulate the size of the domains. For example, addition of the more symmetric copolymer increases the relative size of the domains with respect to the unit cell volume, because more symmetric diblocks prefer less curved interfaces. Second, the two diblocks could segregate within a domain, providing a mechanism to regulate the shape of the domains. That is, the interface region with higher concentration of the more asymmetric copolymers would have a larger curvature, resulting

in nonspherical domains. The formation of minority domains with different sizes and shapes would be beneficial to the formation of the FK phases.

The availability of the SCFT solutions for different ordered phases allows a quantitative examination of the suggested mechanisms related to the segregation of the two diblocks. Specifically, the local concentration and segment distribution could be computed from the propagators, which are solutions of the modified diffusion equations in the self-consistent fields.<sup>22,26,27</sup> In order to be specific, we focus on a line of  $\gamma = 1.7$  in the phase diagram shown in Figure 2a, along with the stable phase of the binary blends changes from BCC to the  $\sigma$  and finally to the cylindrical (C) phase as the total concentration of  $A_1B_1$  is decreased from 1 to 0.5. At each concentration, the volume of the five different domains and the local concentration of  $A_1$  block within each domain are calculated from the SCFT solutions. The results are presented in Figure 4.

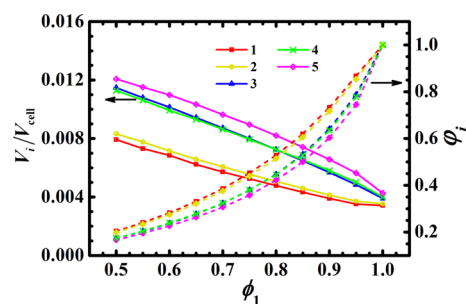


**Figure 4.** Volume  $V_i$  of five nonequivalent domains relative to the unit-cell volume  $V_{\text{cell}}$ ,  $V_i/V_{\text{cell}}$  ( $i = 1, 2, \dots, 5$ ), and concentrations of the  $A_1$  blocks inside these domains,  $\phi_i$ , for the  $\sigma$  phase, as a function of  $\phi_1$  along the phase path of  $\gamma = 1.7$  in Figure 2a.

The volume  $V_i$  of the  $i$ th domain is measured by the volume inside the density isosurface at  $\phi_A(\mathbf{r}) = 0.5$ . An obvious result shown in Figure 4 is that, generically, all the minority domains become larger when  $\phi_1$  is decreased from  $\phi_1 = 1$  or when more longer  $A_2B_2$  diblocks are added. This result is consistent with the argument that larger domain sizes would favor the formation of complex spherical phases. In addition, the local concentration of  $A_1$  blocks within each domain,  $\phi_i$ , reveals that the size of different domains is correlated with the concentration. These results provide direct evidence that the redistribution of the different diblock copolymers drives the formation of domains with different sizes, thus facilitating the formation of the complex FK phases.

We now turn to the segregation of the two different diblocks within each domain and present a quantitative correlation between their local segregation and nonsphericity of the domains. The basic idea is that, if the two diblock copolymers are randomly mixed at the interfaces, the interfaces would have a constant spontaneous curvature favoring the formation of spherical domains. Deformation of these spherical domains would have an energetic penalty. On the other hand, the segregation of the two diblocks at the interfaces would lead to inhomogeneous interfacial curvature favoring the formation of nonspherical domains. Therefore, segregation of block copolymers within a domain provides a mechanism to regulate its shape. A calculation of the local concentration of the different diblocks at the interfaces would provide direct evidence of this mechanism. Thus, the distribution of the joint point of  $A_1B_1$ ,  $\phi_1 q(\mathbf{r}, f_1) q^\dagger(\mathbf{r}, f_1)/Q_1$ , at the A/B interfaces

at  $\gamma = 1.7$  and  $\phi_1 = 0.6$ , has been calculated. At this point of the phase space,  $f_1 = 0.15$  for  $A_1B_1$  and  $f_2 = 0.5$  for  $A_2B_2$ , and the  $\sigma$  phase is the equilibrium one. The density profile of the joint points along the interfaces is presented in Figure 3b,c for the five types of domains, which indicates that the distribution of the diblocks at the interfaces is noticeably nonuniform. The results directly reveal that the more asymmetric  $A_1B_1$  diblocks are segregated to the regions of higher curvatures, whereas the more symmetric  $A_2B_2$  diblocks are more enriched in the lower curvature area. The nonuniform copolymer distribution correlates perfectly with the local curvature of the interfaces.

In conclusion, the phase behavior of binary mixtures of  $AB$  diblock copolymers has been examined using extensive SCFT calculations. Phase diagrams of the binary blends in the interested phase space have been constructed (Figure 2 for  $\chi N = 40$  and Figure S3 for  $\chi N = 20$ ). Starting from a BCC-forming diblock copolymer, it is discovered that the addition of a small amount of a second diblock copolymer with longer minority  $A$ -blocks leads to the formation of the FK phases. In particular, for a diblock copolymers with  $\chi N = 40$  and  $f = 0.15$ , the addition of a second diblock with longer  $A$  blocks results in a phase transition sequence of  $BCC \rightarrow \sigma \rightarrow A15 \rightarrow C$  (e.g., Figure 2 with  $\gamma = 1.9$ ). It is interesting to note that this phase sequence is generally observed in a number of soft matter systems.<sup>3–7</sup> The phase diagrams exhibit a surprisingly large stable region for the  $\sigma$  phase. These theoretical predictions not only demonstrate the proposed formation mechanism of the FK phases by Bates and co-workers<sup>7</sup> in a quantitative manner, but also suggest a robust yet simple route to obtain the complex FK phases using simple binary blends, in contrast to traditional routes using specifically synthesized block copolymers. In particular, the redistribution of the diblock copolymers via local segregation plays a dual role in controlling the domain size and shape. The segregation among different domains favors the formation of domains of different sizes, whereas the segregation within a domain helps the formation of domains with nonspherical shapes.

Note that the formation of the  $\sigma$  phase in pure copolymer systems usually needs a long annealing time for the process of mass exchange between domains.<sup>6,7</sup> Importantly, our results in Figures 2 and S3 suggest that the formation of the  $\sigma$  phase in the binary blend is insensitive to the segregation degree. This implies that the kinetics of mass exchange could be speeded up by increasing the diffusion constant of polymer chain via lowering molecular weights. Furthermore, for the copolymers with temperature-insensitive  $\chi$  (e.g., PS-*b*-PMMA), the diffusion constant can be increased further by raising the annealing temperature without changing the stability region of the desired  $\sigma$  phase. In brief, the concept that the self-assembly of tailored polydisperse block copolymers leads to the formation of complex ordered phases can be extended to other complex structures, for example, bicontinuous network structures beyond the gyroid phase.<sup>30–32</sup>

## ■ ASSOCIATED CONTENT

### ● Supporting Information

The Supporting Information is available free of charge on the ACS Publications website at DOI: 10.1021/acsmacrolett.6b00685.

Further description and figures regarding the self-consistent field theory, the comparisons of free energy, typical density profiles, the phase sequence, and the IQ of five types of (non)spherical domains (PDF).

## ■ AUTHOR INFORMATION

### Corresponding Authors

\*E-mail: weihuali@fudan.edu.cn.

\*E-mail: shi@mcmaster.ca.

### Notes

The authors declare no competing financial interest.

## ■ ACKNOWLEDGMENTS

The authors gratefully acknowledge helpful discussions with Prof. Müller. This work was supported by the National Natural Science Foundation of China (21322407, 21574026, and 2014M560289); A.-C.S. acknowledges the support from the Natural Science and Engineering Research Council (NSERC) of Canada.

## ■ REFERENCES

- (1) De Graef, M.; McHenry, M. E. *Structure of Materials: An Introduction to Crystallography, Diffraction, and Symmetry*, 2nd ed.; Cambridge University Press: New York, 2012.
- (2) Frank, F. C.; Kasper, J. S. *Acta Crystallogr.* **1959**, *12*, 483–499.
- (3) Ungar, G.; Liu, Y. S.; Zeng, X. B.; Percec, V.; Cho, W. D. *Science* **2003**, *299*, 1208–1211.
- (4) Zeng, X. B.; Ungar, G.; Liu, Y. S.; Percec, V.; Dulcey, A. E.; Hobbs, J. K. *Nature* **2004**, *428*, 157–160.
- (5) Huang, M.; Hsu, C.-H.; Wang, J.; Mei, S.; Dong, X.; Li, Y.; Li, M.; Liu, H.; Zhang, W.; Aida, T.; Zhang, W.-B.; Yue, K.; Cheng, S. Z. D. *Science* **2015**, *348*, 424–428.
- (6) Lee, S. W.; Bluemle, M. J.; Bates, F. S. *Science* **2010**, *330*, 349–353.
- (7) Lee, S. W.; Leighton, C.; Bates, F. S. *Proc. Natl. Acad. Sci. U. S. A.* **2014**, *111*, 17723–17731.
- (8) Grason, G. M.; DiDonna, B. A.; Kamien, R. D. *Phys. Rev. Lett.* **2003**, *91*, 058304.
- (9) Xie, N.; Li, W. H.; Qiu, F.; Shi, A. C. *ACS Macro Lett.* **2014**, *3*, 906–910.
- (10) Chanpuriya, S.; Kim, K.; Zhang, J.; Lee, S.; Arora, A.; Dorfman, K. D.; Delaney, K. T.; Fredrickson, G. H.; Bates, F. S. *ACS Nano* **2016**, *10*, 4961–4972.
- (11) Gillard, T. M.; Lee, S.; Bates, F. S. *Proc. Natl. Acad. Sci. U. S. A.* **2016**, *113*, 5167–5172.
- (12) Liu, M. J.; Li, W. H.; Qiu, F.; Shi, A.-C. *Soft Matter* **2016**, *12*, 6412–6421.
- (13) Zihlerl, P.; Kamien, R. D. *Phys. Rev. Lett.* **2000**, *85*, 3528–3531.
- (14) Zhang, J. W.; Bates, F. S. *J. Am. Chem. Soc.* **2012**, *134*, 7636–7639.
- (15) Hashimoto, T.; Koizumi, S.; Hasegawa, H. *Macromolecules* **1994**, *27*, 1562–1570.
- (16) Yamaguchi, D.; Takenaka, M.; Hasegawa, H.; Hashimoto, T. *Macromolecules* **2001**, *34*, 1707–1719.
- (17) Court, F.; Hashimoto, T. *Macromolecules* **2002**, *35*, 2566–2575.
- (18) Shi, A. C.; Noolandi, J. *Macromolecules* **1995**, *28*, 3103–3109.
- (19) Matsen, M. W.; Bates, F. S. *Macromolecules* **1995**, *28*, 7298–7300.
- (20) Wu, Z. Q.; Li, B. H.; Jin, Q. H.; Ding, D. T.; Shi, A. C. *Macromolecules* **2011**, *44*, 1680–1694.
- (21) Matsen, M. W.; Schick, M. *Phys. Rev. Lett.* **1994**, *72*, 2660–2663.
- (22) Matsen, M. W. *J. Phys.: Condens. Matter* **2002**, *14*, R21–R47.
- (23) Arora, A.; Qin, J.; Morse, D. C.; Delaney, K. T.; Glenn, H.; Bates, F. S.; Dorfman, K. D. *Macromolecules* **2016**, *49*, 4675–4690.
- (24) Tzeremes, G.; Rasmussen, K.; Lookman, T.; Saxena, A. *Phys. Rev. E: Stat. Phys., Plasmas, Fluids, Relat. Interdiscip. Top.* **2002**, *65*, 041806.
- (25) Rasmussen, K. Ø.; Kalosakas, G. J. *Polym. Sci., Part B: Polym. Phys.* **2002**, *40*, 1777–1783.
- (26) Fredrickson, G. H. *The Equilibrium Theory of Inhomogeneous Polymers*; Clarendon Press: Oxford, 2006.

- (27) Shi, A.-C. Self-Consistent Field Theory of Block Copolymers. In *Dev. Block Copolym. Sci. Technol.*; John Wiley & Sons, Ltd, 2004; pp 265–293.
- (28) Matsen, M. W. *Phys. Rev. Lett.* **2007**, *99*, 148304.
- (29) Milner, S. T.; Witten, T. A.; Cates, M. E. *Macromolecules* **1989**, *22*, 853–861.
- (30) Matsen, M. W. *Macromolecules* **2012**, *45*, 2161–2165.
- (31) Müller, M.; Sun, D.-W. *Phys. Rev. Lett.* **2013**, *111*, 267801.
- (32) Wang, X. B.; Lo, T. Y.; Hsueh, H. Y.; Ho, R. M. *Macromolecules* **2013**, *46*, 2997–3004.